COMPARISON OF CRACK-RESISTANCE-CURVES OF WIDE PLATES AND FRACTURE MECHANICS SPECIMENS

A. Liessem*, R. Hubo*, R. Twickler*, W. Dahl*

The calculated plastic collapse load using the EPRI-approach is compared with the experimentally determined plastic collapse load. The influence of different approximations of the stress-strain-curve by the Ramberg-Osgood-equation and the problem of a geometry independent crack resistance curve will be discussed. In order to examine the question if the J-Δa-curve of sidegrooved 1CT25-specimens can be used as a lower bound curve crack resistance curves on wide plates were determined and compared with those of fracture mechanics specimens.

INTRODUCTION

The evaluation of the maximum load bearing capacity of cracked components for ductile material behaviour can be performed based on crack resistance curves determined in fracture mechanics tests. This procedure is included e.g. in the EPRI-approach. A comparison of calculated and experimentally determined plastic collapse loads shows an overestimation of the experimental loads up to 10% although a "lower bound" J-Δa-curve of sidegrooved 1CT25-specimens has been used.

The Ramberg-Osgood-equation for approximation of the stress-strain-curve of steels with Lueders plateau is one reason for the misfit. The extrapolation of the J-Δa-curve to larger amounts of crack extension being observed in the wide plates is another problem of a failure analysis based on the J-Δa-curve-approach.

In connection with the "lower bound" crack resistance curve problem J-Δa-curves of wide plates have been evaluated. A special testing procedure has been developed including J-contour-measurements and ACPD-monitoring to observe stable crack extension. The experimentally determined J_{appl}-values show a good agreement with calculated J_{appl}-values using Finite-Element-Calculations. The comparison of J-Δa-curves of wide plates and sidegrooved 1CT25-specimens showed much higher J-values for the wide-plate-curve. For failure assessment of relatively thin DECT-specimens therefore the J-Δa-curves of the small scale specimens can be used as a lo-

* Institute of Ferrous Metallurgy, Technical University of Aachen, Aachen, F.R.G.

wer bound curve. The investigations have been performed with five different steels of grade FeE 355, FeE 690, and FeE 885.

APPLICATION OF THE EPRI-APPROACH

For the assessment of the failure behaviour of structures containing flaws different fracture mechanics based concepts are developed comparing material properties and applied crack driving force. A numerical method to assess the structural integrity is the EPRI-approach from Kumar et al. (1) which provides a simplified methodology to predict the fracture of flawed structural components for elastic-plastic and fully plastic material and component behaviour. This engineering approach allows a calculation of the driving force J_{appl} as a function of the external load for a variety of flawed structural geometries. In the EPRI-handbook, different solutions for the calculation of J_{appl} are given derived from extensive FE-calculations for various configurations. These solutions are calculated for plane stress and plane strain situations. The stress-strain-curve can be described using the Ramberg-Osgood-relationship.

Comparing the driving force J_{appl} consisting of an elastic and a plastic share with values determined on fracture mechanics specimens (J_c, J_i and J-Δa) failure loads of components can be evaluated. This procedure is shown in figure 1. The J-integral is shown as a function of crack length. The J_{appl}-curves are shifted to higher J-values with increasing load and constant crack length. Above net section yielding the J-values increase rapidly. The load at initiation of stable crack extension can be derived from the intersection of the J_i-material value and the J_{appl}-curves. Figure 2 shows a comparison of calculated and experimentally determined initiation stresses of the wide plate tests. Independent of the material strength, the σ_i values are in good agreement with a maximum derivation of ± 5%. Based on this results the evaluation of initiation stresses seems to be quite uncomplicated.

The instability load (plastic collapse load) is given by the equation

$$\frac{\delta J_{appl}}{\delta a} = \frac{\delta J_R}{\delta a} \qquad (1)$$

Depending on the crack resistance curve (see figure 1, No. 1 or No. 2, assumed curves with different initiation and crack extension behaviour) significant differences of the plastic collapse loads and the ductile tearing up to collapse are evaluated.

The following essential requirements for the application of the EPRI-approach have to be respected in particular for instability load determination:

I. The stress-strain behaviour has to be described by a Ramberg-Osgood-relationsship,
II. A geometry independent J-Δa-curve is required valid for plane strain conditions.

The description of the yielding behaviour of steels with Lueders plateau by a Ramberg-Osgood-law gives some difficulties. The single regimes of the stress-strain-curve can be taken into account more or less accurate. The constants α and N of the power law have a strong influence on the result, with greater α-values and small N-values describing the plastic regime quite well, whereas the best fit for the elastic regime is given by small α-values and great Nvalues.

If preference is given to the plastic behaviour, in general better predictions of plastic collapse loads are received.

An other difficulty using this procedure is included in the second requirement. If a fracture mechanics crack resistance curve determined with small scale specimens is used and large amounts of stable crack extension as determined in wide plates tests have to be assessed, this can result in a problem, because the J-Δa-curve has to be extrapolated to higher Δa-and J-values. Consequently the calculation of plastic collapse loads depends on the kind of extrapolation in a significant way.

In spite of these problems the EPRI-approach has been applied to the wide plate geometries and the test results were used for the assessment of the calculated collapse loads.

The crack resistance curves determined on small scale specimens were approximated by a power law function $y = a \cdot x^b$ and applied beyond the validity of J-controlled crack extension. For the approximation of the true-stress-true strain-curve, two different starting points were chosen in order to describe either the elastic or the plastic behaviour in a better way.

The comparison of the calculated collapse loads with the measured ultimate loads is shown in figure 3. Irrespective of the crack ratio 2a/W, the specimen geometry, the strength of the steel and the kind of approximation the maximum scatter amounts to 10%. This result agrees well with the conclusions of former investigations (2), in which non-conservative predictions of plastic collapse loads are evaluated as well in some cases for wide plates of steels exhibiting a Lueders plateau. This problem gives the background for this investigation, which should show the influence of constraint in small and large scale specimens on the crack resistance curves. It should also be demonstrated, that the crack resistance curve of small scale specimens can be used as a "lower-bound" curve for safety assessments.

Material and testing procedure

The investigations have been performed with 30 mm thick steel plate of grade FeE 355D, FeE 355DD, FeE 690 and two steels of grade FeE 885 (I and II). The chemical composition is given in table 1. The FeE 355DD shows a lower carbon content and small amounts of microalloying elements compared to the conventional FeE 355D steel. In contrast to the normalized and thermomechanically treated FeE 355 steels the high strength steels are quenched and tempered. The main alloying elements are Cr and Mo for the FeE 690 and Ni, Cr and Mo for the highest strength steels FeE 885. The strength values and the results of Charpy-V-tests at room temperature are given in table 2. Yield strength values between 380 MPa (FeE 355DD) and 1005 MPa (FeE 885) have been evaluated in uniaxial tensile tests. The Charpy-V-tests (upper transition range or upper shelf values) revealed values between 80J (FeE 355D) and 280 J (FeE 355DD).

Fracture mechanics crack resistance curves (J-Δa-curves) have been evaluated by multi-specimen-technique using 20% sidegrooved 1CT25-specimens. A power law of the type $y = a \cdot x^b$ has been used for the approximation of the data points. The J-integral values have been evaluated according to ASTM E 813-81 (3).
The initiation of stable crack extension has been determined by DCPD-technique (direct current potential drop).

The orientation of the large and the small scale specimens was transverse to the rolling direction of the original plates (T-L). The thickness of the wide plates was 30 mm and identical with the original plate thickness. The wide plates had a width of 300 mm and an overall length of 2600 mm.

Double edge cracked plates (DECT-double-edge-cracked-tension) with a crack ration 2a/W = 0.2 have been tested. Investigations of Ehrhardt (2) showed that the smallest difference between plastic limit load (net section yielding) and plastic collapse load (maximum load after ductile tearing) is observed for this kind of crack geometry and crack ratio so that the most critical plastic collapse situation has been analysed.

Stable crack extension in the wide plates has been evaluated by ACPD-technique (alternating-current-potential-drop). Current and potential leads were identical with those used for the 1CT25-specimens (see fig.4.).

The driving force in the wide plate has been evaluated in terms of the J-integral by strain gage measurements along a special contour. This has been done according to previous investigations in USA and Japan (4-6). Figure 4 shows the contour Γ and the position of the measuring equipment. The deformation of the DECT-specimens is concentrated in the area between the two crack tips (2). Therefore strain gages with a higher strain capacity (up to 10%) have been used in this area whereas lower strain capacity gages (5%) have been applicated along the further contour. The data of the linear transducers and the clip gage on the edge of the wide plate (COD measurement) have been included in the J-integral-calculation.

The crack resistance curves of the wide plates can be arranged from the potential drop measurements, leading to a calibration curve, and the J-contour measurements as demonstrated in figure 5.

The experimentally determined J-values (J_{appl}) are shown in figure 6 as a function of the external load in terms of the gross section stress. The J-values increase only slightly with increasing stress for elastic specimen behaviour. After net-section-yielding they arise very strongly whereas the gross section stress nearly remains on the same level. One effect results from the Lueders plateau in the stress-strain behaviour of these steels.

The comparison of experimental J_{appl}-curves for the steels FeE 355D and FeE 690 and the J_{appl}-curves calculated by Finite-Element-computations under plane stress conditions shows good agreement up to initiation of stable crack extension and also above this point. The experimental J_{appl}-curves for the FeE 885 wide plates showed higher J-values under the elastic loading conditions. This results from the different crack lengthes on both sides of the wide plate (a_o = 18 mm and a_o = 31 mm). The J-integral has been determined on a contour around the longer crack tip, at which the tensile load is superposed by an additional bending moment leading to a higher loading situation at the crack tip. After net section yielding the additional bending moment can be compensated by plastic deformation so that the difference between experimental and calculated J-values decreases.

Influence of constraint on crack resistance curves

The influence of constraint on the crack resistance curve is discussed based on a direct comparison of the J-Δa-curves of small and large scale specimens of equal thickness. Figure 7 shows the comparison for the steels FeE 690 and FeE 885 I and II. The J_i-value of the wide plate of the steel FeE 690 is smaller than determined in the fracture mechanism investigations whereas the steels FeE 885 I shows a higher value in the wide plate. In general, the differences are small and result from the difficulties in the determination of the initiation point from the ACPD-curve. The good agreement between J_i-values from large and small scale specimens indicates a very similar local constraint at initiation, which is very near to a plane strain situation not only in the sidegrooved 1CT25-specimen but also in the wide plate.

This result has also been derived from other investigations (8-10), in which similarity of the constraint has also been demonstrated by results form Finite-Element-computations.

Large differences between the J-Δa-curves of small and large scale specimens were observed after crack initiation. At the same amount of crack extension Δa the J-values are higher in the wide plates, resulting from a different change of the constraint in the specimens. The local constraint in the small scale specimens is supposed to remain constant after initiation due to only small plastic deformations and sidegrooves which counteract any change of constraint, so that the plane strain situation is active also during crack extension. This supposition has been prooved by numerical investigations (11,12). The local constraint in the wide plate is decreased due to large plastic deformations ahead of the crack tip. To reach the critical plastic strain for crack extension, which depends directly on the constraint, therefore needs higher loads, so that the same amount of Δa is observed at higher J-values.

The result of the comparison of J-Δa-curves between large and small scale specimens is of significance for a fracture mechanics safety analysis. In general, the crack resistance curve of the sidegrooved 1CT25-specimens is used as a lower bound curve. This statement is restricted on rather thin structures, because experimental investigations on the crack extension behaviour of thick wide plates and geometries with large defect ratios have shown, that in special cases J-Δa-curves are obtained with a slope lower than determined on sidegrooved 1CT25-specimens (13). Numerical investigations revealed that a diminution of the constraint in front of the crack tip after plastic deformation appears in both the small and the large scale specimens. The ratio of the plastic zone to the undeformed ligament is very small in the small scale specimen under plane strain conditions, so that the diminution of the constraint situation has only a local effect whereas the whole cross section in the wide plate is strongly influenced by plastic deformation and change of constraint. The steel FeE 355DD (see figure 8.) reveals the same behaviour as the high strength steels FeE 690 and FeE 885.

Steel FeE 355D shows only insignificant higher J-values for the J-Δa-curve of the wide plate, but only for high Δa-values. This indicates a generally low crack resistance of this steel. The J-Δa-curves of the wide plate and the 1CT25-specimen are almost identical. If the assumptions for the explanation of the differences in the crack extension behaviour between wide plate and fracture mechanics specimen established for steels FeE 690, FeE 885 I and II and FeE 355DD are correct, one can conclude, that the change of constraint due to plastic deformation is not developed in steel FeE 355D due to extensive crack extension which can not be compensated by plastic deformation and strain hardening. The influence of the change of constraint during crack extension therefore is not only dependent of the geometry but also of the absolute level of toughness. Similar results were obtained with investigations of thicker wide plates (13).

Conclusion

The crack resistance behaviour of steels with different strength (FeE 355 to FeE 885) has been examined with fracture mechanics specimens and wide plates (plate thickness: 30 mm), in order to determine the influence of constraint on the initiation and the crack extension behaviour. The fracture mechanics crack resistance curves (J-Δacurves) were evaluated with the multiple-specimen-technique. The set up for the J-Δa-curves of wide plates was carried out by ACPD-monitoring and experimentally determined J-values. The wide plates showed steeper J-Δa-curves than the 20% sidegrooved 1CT-specimens, so that for the use in safety analysis of this structures the J-Δa-curves of the small specimens can be considered as a "lower bound". The lower constraint in the wide plates after crack initiation results in a steeper J-Δa-curve. However this can only be observed in case of generally sufficient toughness and only then can be taken into account as a safety reserve in a failure analysis of components.

References

(1) Kumar, V., M.D. German und C.F. Shih: An Engineering Approach for Elastic-Plastic Fracture Analysis, Electric Power Research Institute (EPRI) NP 1931, Project 1237-1, Final Report, General Electric Company, Schenectady, N.Y. 12301

(2) Ehrhardt, H.: Investigations on the influence of different defect geometries on the failure behaviour of steels based on wide plate tests, PhD-thesis (german), Technical University Aachen, 1989

(3) ASTM: Standard test method for J_{Ic}, a measure of fracture toughness, American Society for Testing and Materials, ASTM E 813-81, Annual Book of ASTM-Standards, Philadelphia, USA, 1981

(4) Read, D.T.: Experimental Method for Direct Evaluation of the J-Contour Integral, in: ASTM STP 791, eds: J.C. Lewis and G. Sines, American Society for Testing and Materials, Philadelphia, USA, 1983, pp. II.199-II.213

(5) Kawahara, W.A. und S.L. Brandon: J-Integral Evaluation by resistance strain ganges, Eng. Frac. Mech. Vol. 18, No. 2, S. 427-434, 1983

(6) Dodds, R.H. and D.T. Read: Experimental and analytical estimates of the J-integral for tensile panels containing short center cracks, Int. J. Frac. 28 (1985), S. 39-54

(7) Hubo, R.: Fracture mechanics investigations for the use of steels of different strength and toughness, PhD-thesis (german), Technical University Aachen, 1990

(8) Aurich, D., K. Wobst und H. Krafka: J_R-Curves of wide plates and CT25-specimens; Comparison of the results of a pressure vessel, in: proc. 13. MPA-seminar, volume 2, pp. 46.1-46.20, University Stuttgart 1987

(9) Eisele, U., E. Roos: Valuation of different J-integral initiation values with regard to their usability in the safety assessment of components, in: proc. 15. MPA-seminar, volume 2, pp. 38.1-38.23, University Stuttgart 1989

(10) Roos, E., H. Silcher, U. Eisele: On "lower bound crack resistance curves" as a material law for the safety assessment of components, in: proc. 15. MPA-seminar, volume 2, pp. 39.1-39.18, University Stuttgart 1989

(11) Aurich, D.: Analyse und Weiterentwicklung bruchmechanischer Versagenskonzepte auf der Grundlage von Forschungsergebnissen auf dem Gebiet der Komponentensicherheit: Teilvorhaben BAM-Berlin, Entwurf des Abschlußberichtes, BAM, Berlin 1989

(12) Schmitt, W.: Analyse und Weiterentwicklung bruchmechanischer Versagenskonzepte auf der Grundlage von Forschungsergebnissen auf dem Gebiet der Komponentensicherheit: Teilvorhaben IWM-Freiburg, Entwurf des Abschlußberichtes, IWM, Freiburg 1989

(13) Clausmeyer, H., K. Kussmaul und E. Roos: Der Einfluß des Spannungszustandes auf den Versagensablauf angerissener Bauteile aus Stahl, Mat. wiss. u. Werkstofftech. 20 (1989), S. 101-117

TABLE 1 - Chemical composition of the steels

Steel	C	Si	Mn	P	S	N	Al	Cu	Cr	Ni	Mo	V	Nb
FeE 355D	0.15	0.38	1.54	0.016	0.021	0.011	0.024	0.035	0.005	0.035	0.005	0.039	0.001
FeE 355DD	0.11	0.34	1.66	0.008	0.002	n.d.	0.006	0.287	0.052	0.264	0.032	0.006	0.019
FeE 690	0.18	0.61	0.95	0.013	0.004	n.d.	0.066	n.d.	0.91	n.d.	0.42	n.d.	n.d.
FeE 885 I	0.16	0.27	0.76	0.007	0.001	n.d.	0.025	n.d.	0.60	1.87	0.41	0.060	n.d.
FeE 885 II	0.18	0.28	0.78	0.008	0.003	n.d.	0.035	0.086	0.62	1.86	0.44	0.065	0.006

n.d. = non determined

TABLE 2 - Mechanical properties at room temperature

Steel	σ_{YS} MPa	σ_{TS} MPa	σ_{YS}/σ_{TS}	A_5 %	Z %	C_v J
FeE 355D	397	556	0.71	32	71	80
FeE 355DD	380	520	0.73	37	79	280
FeE 690	755	850	0.89	22	74	210
FeE 885 I	1005	1051	0.96	18	66	166
FeE 885 II	1001	1054	0.95	21	68	168

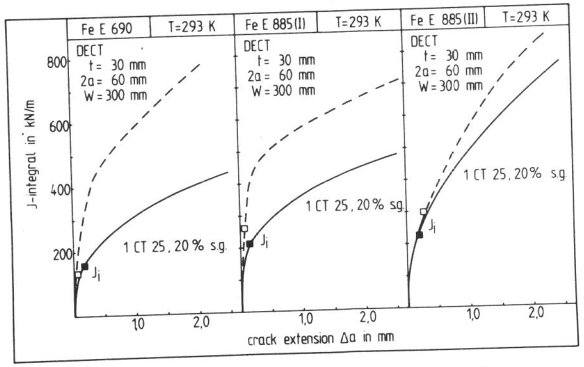

Figure 7 Crack resistance curve of small and large scale specimens (FeE 690, FeE 885I, FeE 885II)

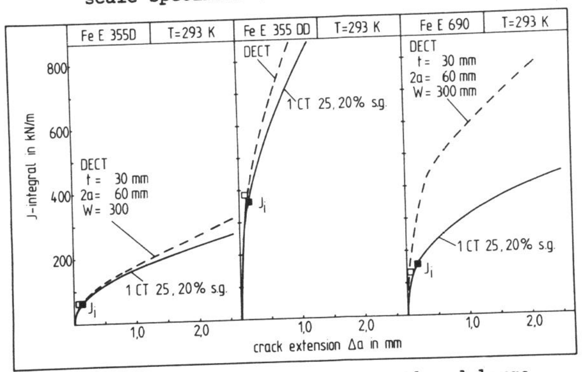

Figure 8 Crack resistance curve of small and large scale specimens (FeE 355D, FeE 355DD, FeE 690)

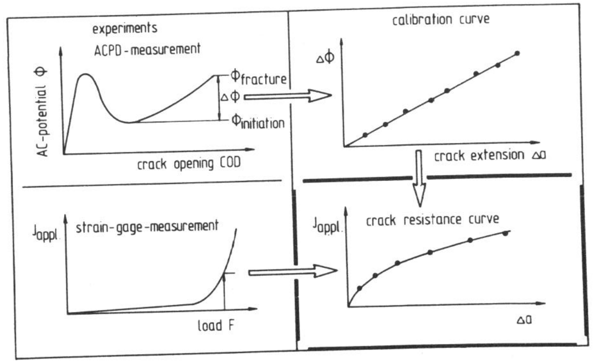

Figure 5 Procedure for evaluation of J-Δa-Curves of wide plates

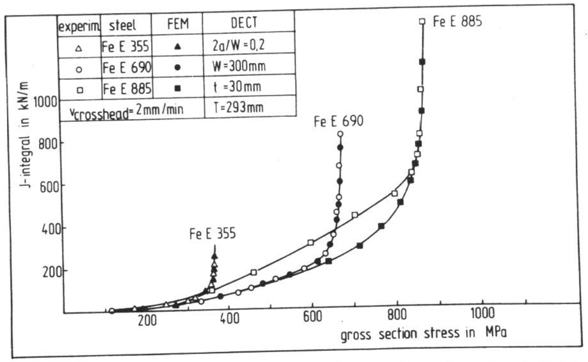

Figure 6 Comparison of experimental and calculated J_{appl}-curves

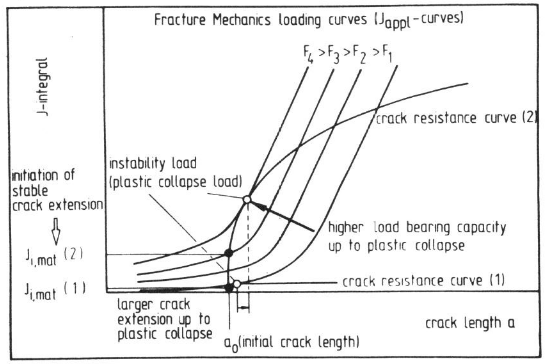

Figure 1 Evaluation of instability loads

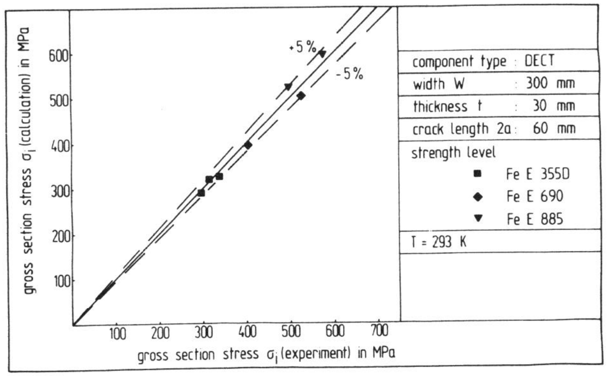

Figure 2 Comparison of predicted and experimentally determined initiation stresses σ_i

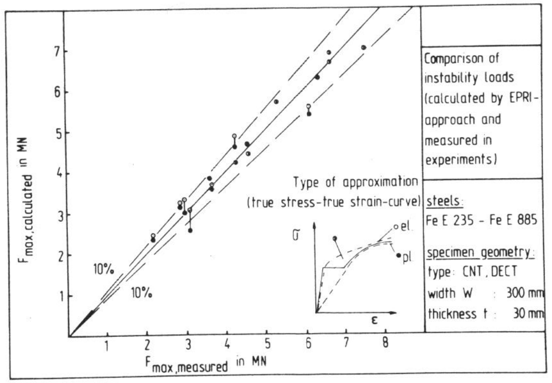

Figure 3 Comparison of instability loads

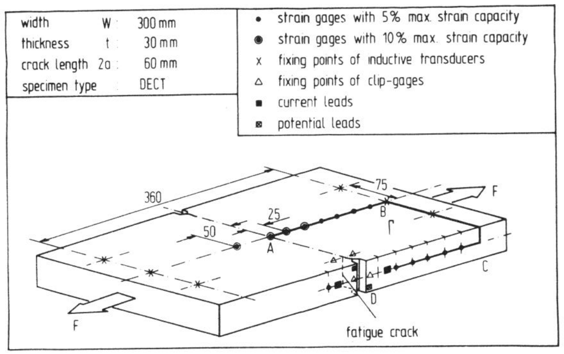

Figure 4 Measuring equipment of wide plate